NACA RM E55A03

NACA

# RESEARCH MEMORANDUM

## INVESTIGATION OF A HIGH-PRESSURE-RATIO EIGHT-STAGE AXIAL-FLOW RESEARCH COMPRESSOR WITH TWO TRANSONIC INLET STAGES

## V - PRELIMINARY ANALYSIS OF OVER-ALL PERFORMANCE OF MODIFIED COMPRESSOR

By Raymond M. Standahar and Richard P. Geye

Lewis Flight Propulsion Laboratory
Cleveland, Ohio

NATIONAL ADVISORY COMMITTEE FOR AERONAUTICS

WASHINGTON

May 23, 1955
Declassified September 17, 1958

NATIONAL ADVISORY COMMITTEE FOR AERONAUTICS

RESEARCH MEMORANDUM

# INVESTIGATION OF A HIGH-PRESSURE-RATIO EIGHT-STAGE AXIAL-FLOW RESEARCH COMPRESSOR WITH TWO TRANSONIC INLET STAGES

## V - PRELIMINARY ANALYSIS OF OVER-ALL PERFORMANCE OF MODIFIED COMPRESSOR

By Raymond M. Standahar and Richard P. Geye

## SUMMARY

An investigation of the over-all performance of a modified eight-stage axial-flow compressor was conducted as part of the investigation of the problems encountered in a high-pressure-ratio axial-flow compressor with transonic inlet stages.

The investigation was made over a range of weight flows at equivalent speeds from 30 to 110 percent of design speed. The maximum total-pressure ratio obtained at design speed was 11.0 at an equivalent weight flow of 70.9 pounds per second with an adiabatic efficiency of 0.81. A maximum equivalent weight flow of approximately 72.5 pounds per second (30.6 lb/(sec)(sq ft of frontal area)) was obtained at design speed. A peak efficiency of 0.67 was obtained at 30 percent of design speed, and as the compressor speed increased, a maximum peak efficiency of approximately 0.85 was obtained at 90 percent design speed. The predicted values of over-all total-pressure ratio and weight flow agree very well with the experimental values obtained at 90 and 100 percent of design speed, while the measured efficiencies at these speeds are 3 to 4 percentage points lower than the predicted values.

## INTRODUCTION

As part of the general program initiated to study the design and off-design performance problems of a high-mass-flow, high-pressure-ratio multistage compressor with both transonic and subsonic stages, a 20-inch-tip diameter, eight-stage axial-flow compressor having two transonic inlet stages was designed, fabricated, and tested at the NACA Lewis laboratory (refs. 1 to 3). This compressor did not reach the design values at design speed (ref. 2), and a blade failure ended the original series of tests. In rebuilding this compressor, several modifications were incorporated in an attempt to improve both the aerodynamic and mechanical characteristics of the compressor. Details of these modifications are presented in reference 4.

The initial phase of the investigation of the modified compressor consisted in obtaining the over-all performance characteristics over a range of equivalent speeds from 30 to 110 percent of design speed. The present report discusses the preliminary analysis of the over-all performance on the basis of total-pressure ratio, adiabatic temperature-rise efficiency, and average compressor-discharge Mach number plotted against inlet equivalent weight flow. Stage static-pressure ratios at the tip are presented in order to obtain an indication of the performance of the individual stages over the speed and weight-flow ranges investigated. A comparison is also made with the predicted performance values presented in reference 4.

## SYMBOLS

The following symbols are used in this report:

| | |
|---|---|
| A | area, sq ft |
| P | absolute total pressure, lb/sq ft |
| p | absolute static pressure, lb/sq ft |
| Re | Reynolds number relative to first rotor |
| T | total temperature, $^{o}F$ |
| W | weight flow, lb/sec |
| $\delta$ | ratio of inlet total pressure to NACA standard sea-level pressure |
| $\eta$ | adiabatic temperature-rise efficiency |
| $\theta$ | ratio of inlet total temperature to NACA standard sea-level temperature |

Subscripts:

| | |
|---|---|
| 0 | inlet depression-tank station |
| 20 | discharge measuring station |

## APPARATUS

Compressor. - A photograph of the modified compressor rotor is shown in figure 1, and a cross-sectional view of the compressor, the inlet bellmouth nozzle, and the discharge collector is shown in figure 2. The aerodynamic design details of the compressor are presented in references 1 and 4. The major design values are:

| | |
|---|---|
| Total-pressure ratio | 10.26 |
| Root-mean total-pressure ratio per stage | 1.338 |
| Equivalent weight flow, lb/sec | 72.4 |
| Equivalent weight flow, lb/(sec)(sq ft frontal area) | 30.5 |
| Equivalent tip speed, ft/sec | 1218 |
| Inlet hub-tip ratio | 0.46 |
| Diameter at inlet to first rotor, in. | 20.86 |

Installation. - The compressor was driven by a 9000-horsepower variable-frequency electric motor. The speed was maintained constant by an electronic control and was measured by an electric chronometric tachometer.

Air entered the compressor through a calibrated, adjustable submerged orifice, a butterfly inlet throttle, and a depression tank 6 feet in diameter and approximately 10 feet long. Screens in the depression tank and a bellmouth nozzle faired into the compressor inlet were used to obtain a uniform distribution of air entering the compressor. Air was discharged from the compressor into a collector that was connected to the laboratory altitude exhaust system. Air weight flow at a constant speed was controlled by a butterfly valve located in the exhaust ducting.

Instrumentation. - The axial locations of the instrument-measuring stations are shown in figure 2. The inlet-depression-tank station and the compressor discharge had axial locations that were in accordance with reference 5. Radial distributions of outlet total temperature and total pressure were obtained from multiple-probe rakes located at area centers of equal-annular area. The instrument used at each station and the method of measurement were as follows:

Depression-tank pressure:
Five wall static-pressure taps spaced around the tank circumference

Depression-tank temperature:
Four multiple-tip total-temperature probes

Compressor-inlet static pressure:
Four wall static-pressure taps located around the casing circumference, and two located in the hub approximately 0.5 inch upstream of the first rotor

Compressor-blade-row static pressure:
Four wall static-pressure taps located around the casing circumference after each blade row

Compressor-discharge pressure:
Four wall static-pressure taps at the tip and two at the hub; three 10-tube circumferential total-pressure rakes (fig. 3(a)) located at area centers of equal-annular area. The circumferential length of a rake was greater than the circumferential distance between exit guide vanes.

Compressor-discharge temperature:
Four spike-type thermocouple rakes (fig. 3(b)) with three measuring stations located at area centers of equal annular area. The rakes were located circumferentially around the flow passage so as to be out of exit-guide-vane wakes. These thermocouples were connected differentially with the depression-tank thermocouples.

Pressure measurement:
Mercury manometers

Temperature measurement:
Self-balancing potentiometers

Two blades on each row of rotor and stator blades of the compressor were instrumented with strain gages so that the vibratory stress could be measured. A visual picture of the stress level was obtained by the use of an oscilloscope, which was monitored by the operator.

The constant-temperature hot-wire-anemometer system discussed in reference 6 was used to detect rotating stall. Probes were installed after the first and third rotors and the signals were viewed two at a time on a dual-beam cathode-ray oscilloscope. The accuracy of measurement is estimated to be within the following limits: temperature, $\pm 1.0^{\circ}$ F; pressure, $\pm 0.05$ inch mercury; weight flow, $\pm 1.5$ percent; speed, $\pm 0.3$ percent.

## PROCEDURE

The compressor was operated at equivalent speeds corresponding to 30, 50, 60, 70, 80, 90, 100, and 110 percent of design speed. At each speed, the air flows investigated ranged from a maximum flow to a flow at which surge occurred. The inlet pressure was varied to maintain approximately a constant Reynolds number (based on the blade chord at the tip of the first rotor and the air velocities relative to the tip of the first rotor) of 1,200,000 at all speeds except 30 and 50 percent of design speed. Atmospheric inlet air was used for 30 and 50 percent of design speed and refrigerated inlet air was used at all higher speeds to reduce the outlet temperature and the mechanical speed of the compressor for a given equivalent speed. A continuous check was kept on the blade vibration so that operation in regions of high vibratory stress could be kept to a minimum. A visual check of rotating stall was also maintained as the compressor was brought up to speed. It was found that as the rotating stall disappeared, a noticeable drop in the level of blade vibration was obtained. The knee of the surge line is not clearly defined because severe blade vibrations were encountered in this region and it was decided to complete tests of vibration-free operation first. Upon completion of the 110 percent speed run, the blades were checked and several blades in the fourth row of stators were found to be cracked. In general, the

cracks appeared at two different locations on the blade; one extended in an axial direction approximately 1/4 inch above the end of the base fillet and seemed to emanate from deep tool marks. The other crack started at the juncture of the blade-base button and the overhanging section of the blade trailing edge. The tests were then stopped until a new set of blades could be fabricated. To reduce the vibratory stress in the new set of blades, a larger root fillet was used and the base-button diameter was increased so that there was no overhanging section of the blade trailing edge. As a result of the tests being stopped, the data necessary to define the knee in the surge line were not obtained in the present investigation.

## Calculations

30 to 100 percent design speed. - For each flow point at the 30 to 100 percent design speed, the discharge total pressure was obtained by two methods: The measured discharge total pressure was the arithmetic average of three 10-tube circumferential rake measurements taken at the area centers of equal annular areas. The calculated discharge total pressure was obtained by the method presented in reference 5. With this method, a uniform discharge velocity in the axial direction was assumed and the measured values of discharge static pressure, total temperature, weight flow, and area normal to the compressor axis were used to determine the discharge total pressure from the energy and continuity equations. As the assumptions of this method do not credit the compressor for discharge velocity gradients or deviation from axial discharge, the calculated values of discharge total pressure would be expected to be somewhat lower than the measured values. Actually, the two values correlate very well and because of the recommendations of reference 5, only the compressor total-pressure ratio as determined by the calculated discharge total pressure is presented in this report.

The calculated compressor total-pressure ratio was used to determine the isentropic power input. The compressor temperature rise, obtained by taking the arithmetic average of differential temperatures measured between the compressor discharge and the inlet depression tank, was used to determine the actual power input.

110 percent design speed. - For the flow calculations at 110 percent of design speed, the compressor weight flow and pressure ratio are based on visual readings of single manometers that are used mainly for check data and as such are not averaged readings. It was necessary to use these readings at this speed because of a failure in some of the measuring and recording equipment. It is realized that the values presented for this speed are not exact, but since the check data for the previous speeds showed fair agreement with the averaged data, it was felt that inclusion of the data in this report was useful as an indication of the performance achieved.

## RESULTS AND DISCUSSION

### Modified Compressor Performance

Pressure ratio and adiabatic efficiency. - The over-all performance characteristics of the modified compressor are presented in figure 4 as a plot of total-pressure ratio, with the contours of constant efficiency, as a function of the equivalent weight flow. At design speed, a maximum total-pressure ratio of 11.0 (root-mean total-pressure ratio per stage of 1.35) was obtained at an equivalent weight flow of 70.9 pounds per second (29.9 lb/(sec)(sq ft of frontal area)) with an efficiency of 0.81. A peak efficiency of 0.83 was obtained at total-pressure ratios ranging from 8.7 to 10.25 and a maximum weight flow of approximately 72.5 pounds per second (30.6 lb/(sec)(sq ft of frontal area)) was obtained. At an overspeed condition of 110 percent of design speed, a maximum over-all total-pressure ratio of 12.25 was obtained at an equivalent weight flow of 78.0 pounds per second (32.9 lb/(sec)(sq ft of frontal area)) with an efficiency of 0.80. As explained previously, these overspeed values are not based on averaged values and as such should be used only as an indication of the performance.

The slope of the compressor surge line increased slightly from 30 to 70 percent of design speed. Between 70 and 80 percent of design speed, there is an abrupt change in the slope of the surge line and the slope becomes much greater; probably the front stage operation moves out of stall in this speed range. As explained in the section on PROCEDURE, detailed data on the knee in the surge line were not obtained because of the severe vibrations encountered in this region.

The over-all adiabatic temperature-rise efficiency is plotted as a function of equivalent weight flow in figure 5. The peak efficiency at 30 percent of design speed is approximately 0.67. The peak efficiency increases slowly with speed and reaches a maximum value of approximately 0.85 at 90 percent design speed and then drops to 0.83 at design speed and approximately 0.80 at 110 percent of design speed. As shown in figure 4, the constant efficiency contours cover a wide range of pressure ratio for each equivalent speed. At design speed, the efficiency value is above 0.80 for the greater part of the total-pressure ratio curve.

Compressor-discharge Mach number. - The average compressor-discharge Mach number is presented in figure 6 plotted as a function of equivalent weight flow for various equivalent speeds. The surge line runs through the point of minimum Mach number at each speed. The value of discharge Mach number at surge for design speed was about 0.27. This is approximately the same value of discharge Mach number as was obtained with the compressor of reference 2. Although the compressor weight flow is greater than that of reference 2, the pressure ratio and temperature rise are also higher and as a result the discharge Mach number remains about the same.

Compressor stage characteristics. - A typical curve of static-pressure ratio for a single-stage compressor is plotted in figure 7 as a function of equivalent weight flow. The direction of increasing angle of attack and positive stall is to the left of the peak-pressure-ratio point, and the direction of decreasing angle of attack and negative stall is to the right. A plot of stage static-pressure ratio (based on outer-wall static pressures) against equivalent weight flow is presented in figure 8 for the first, fourth, and eighth stage. (The operating range of the various stages obtained at each speed can be considered as a segment, uncorrected for speed, of the typical stage performance curve presented in fig. 7.)

The inlet stage operates on the positive stall side of the peak-pressure-ratio point at speeds up to 80 percent of design speed (fig. 8(a)). At 90 percent of design speed, the inlet stage is operating in the range of the peak efficiency point and at design speed has moved over to the negative stall side of the stage performance curve.

The fourth stage operates on the positive stall side of the peak-pressure-ratio point at speeds up to 70 percent of design speed (fig. 8(b)). At 80 and 90 percent speed, the stage is operating near the maximum efficiency point, while at design speed the stage operation has moved past the point of maximum efficiency towards the negative stall side of the stage performance curve.

The range of operation of the eighth stage (fig. 8(c)) is much greater than either the first or fourth stage for a given change in compressor weight flow. From 30 to 80 percent of design speed, the stage is operating on the negative stall side of the stage performance curve. At 90 percent of design speed, the curve bends over toward the maximum pressure ratio point, while at design speed the curve actually bends over to the positive stall side of the stage performance curve.

These three stages appear to be very well matched at 90 percent of design speed; that is, they are operating near their peak efficiency points simultaneously. As a result, the peak compressor efficiency of approximately 0.85 was obtained at this speed.

## COMPARISON WITH PREDICTED PERFORMANCE

Total-pressure ratio and adiabatic efficiency. - Figure 9 is a plot of the predicted over-all total-pressure ratio against equivalent weight flow of this compressor as determined by the methods described in references 7 and 8. To give a direct comparison between the predicted and experimental results, the measured total-pressure ratio values are also plotted on figure 9. At 90 and 100 percent of design speed, the correlation between the predicted and experimental values is very good. At 80

percent of design speed, the correlation is good except for the experimental pressure ratio at the surge point, which is approximately 0.4 lower than the predicted value. Except for the 30 percent of design speed results, the correlation at speeds lower than 80 percent is not good. At compressor speeds up to 70 percent of design, rotating stall is present in the compressor and the assumptions of reference 8 used in determining the predicted stage performance parameters will not hold. The stage performance characteristics, therefore, will be different, resulting in pressure ratios and weight flow values that differ from the predicted values.

The predicted variation of adiabatic temperature-rise efficiency with equivalent design speed and weight flow is presented in figure 10. The curve for peak experimental adiabatic efficiency is taken from figure 5 and presented here for comparison. The experimental results are lower than the predicted values over the entire range of speeds tested. The variation ranges from about 2.5 percentage points at 90 percent of design speed to approximately 7 percentage points at 70 percent of design speed. Several reasons for this variation, some of which have been mentioned previously, can be given. At the higher rotational speeds, the rotor-blade tips in the first stage were operating at higher relative inlet Mach numbers than the blades used in setting up the predicted stage performance. The root fillets were appreciably increased in the first three stages, which would tend to increase the blade losses, thus lowering the over-all efficiency.

## SUMMARY OF RESULTS

The following results were obtained from an investigation of over-all performance of a modified eight-stage axial-flow compressor.

1. The maximum total-pressure ratio obtained at design speed was 11.0 at an equivalent weight flow of 70.9 pounds per second with an adiabatic efficiency of 0.81.

2. A peak efficiency of 0.83 was obtained for design speed at values of total-pressure ratio varying from 8.7 to 10.25.

3. A maximum equivalent weight flow of approximately 72.5 pounds per second (30.6 lb/(sec)(sq ft of frontal area)) was obtained at design speed.

4. A maximum peak efficiency of 0.67 was obtained at 30 percent of design speed; a maximum peak efficiency of approximately 0.85 was obtained at 90 percent of design speed.

5. The value of discharge Mach number at surge for design speed was about 0.27.

2J

6. Static-pressure data indicate that the first, fourth, and eighth stages are very well matched at 90 percent design speed; that is, they are operating near their peak efficiency points simultaneously.

7. The predicted values of over-all total-pressure ratio and weight flow correlate very well with the experimental values obtained at 90 and 100 percent design speed.

8. The predicted values of adiabatic temperature-rise efficiency are from 2.5 to 7 percentage points higher than the experimental values obtained over the speed range investigated.

Lewis Flight Propulsion Laboratory
National Advisory Committee for Aeronautics
Cleveland, Ohio, January 6, 1955

## REFERENCES

1. Voit, Charles H.: Investigation of a High-Pressure-Ratio Eight-Stage Axial-Flow Research Compressor with Two Transonic Inlet Stages. I - Aerodynamic Design. NACA RM E53I24, 1953.

2. Geye, Richard P., Budinger, Ray E., and Voit, Charles H.: Investigation of a High-Pressure-Ratio Eight-Stage Axial-Flow Research Compressor with Two Transonic Inlet Stages. II - Preliminary Analysis of Over-All Performance. NACA RM E53J06, 1953.

3. Voit, Charles H., and Geye, Richard P.: Investigation of a High-Pressure-Ratio Eight-Stage Axial-Flow Research Compressor with Two Transonic Inlet Stages. III - Individual Stage Performance Characteristics. NACA RM E54H17, 1954.

4. Geye, Richard P., and Voit, Charles H.: Investigation of a High-Pressure-Ratio Eight-Stage Axial-Flow Research Compressor with Two Transonic Inlet Stages. IV - Modification of Aerodynamic Design and Prediction of Performance. NACA RM E55B28, 1955.

5. NACA Subcommittee on Compressors: Standard Procedures for Rating and Testing Multistage Axial-Flow Compressors. NACA TN 1138, 1946.

6. Laurence, James C., and Landes, L. Gene: Auxiliary Equipment and Techniques for Adapting the Constant-Temperature Hot-Wire Anemometer to Specific Problems in Air-Flow Measurements. NACA TN 2843, 1952.

7. Benser, William A.: Analysis of Part-Speed Operation for High-Pressure-Ratio Multistage Axial-Flow Compressors. NACA RM E53I15, 1953.

8. Medeiros, Arthur A., Benser, William A., and Hatch, James E.: Analysis of Off-Design Performance of a 16-Stage Axial-Flow Compressor with Various Blade Modifications. NACA RM E52L03, 1953.

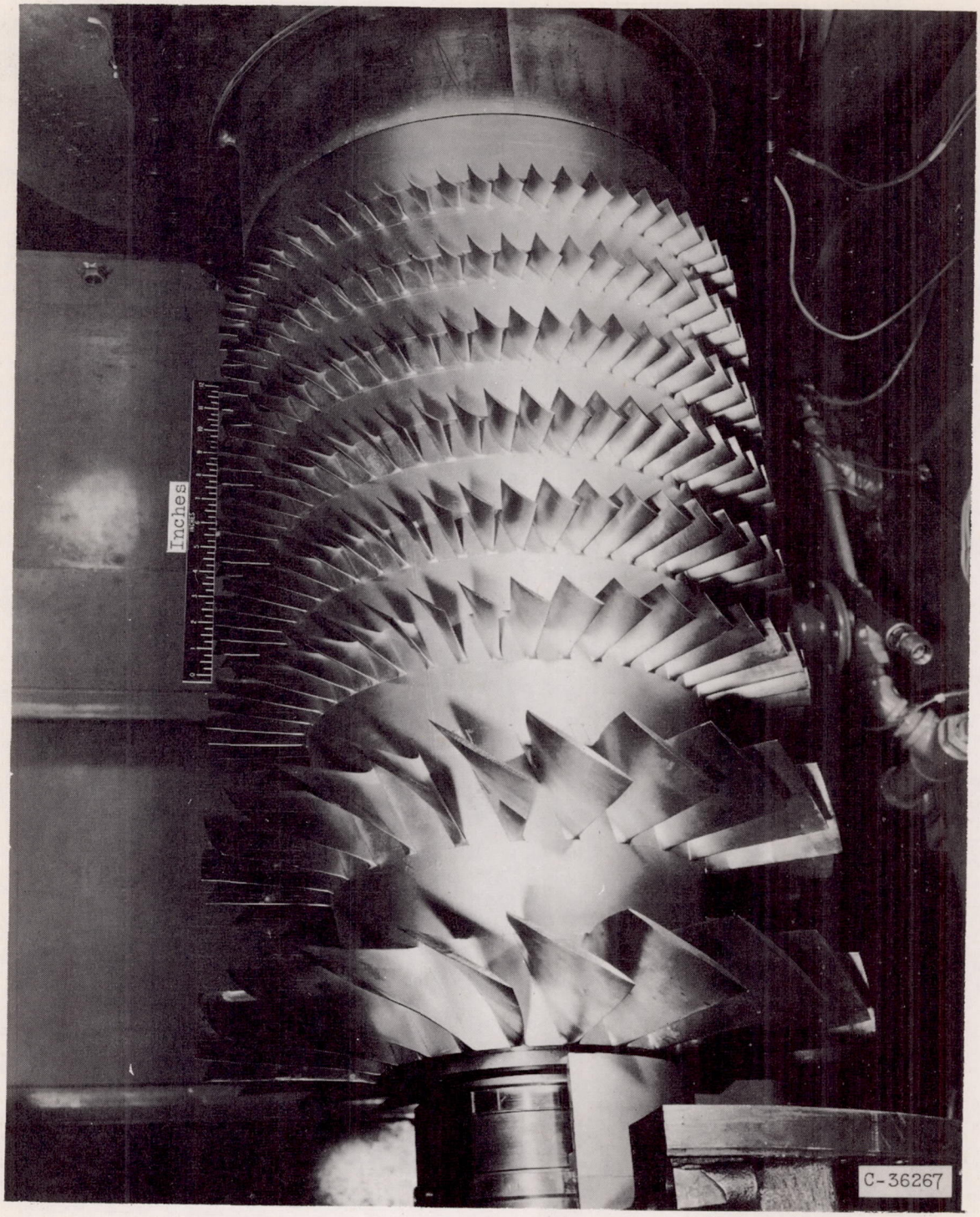



Figure 1. - Modified eight-stage axial-flow compressor.

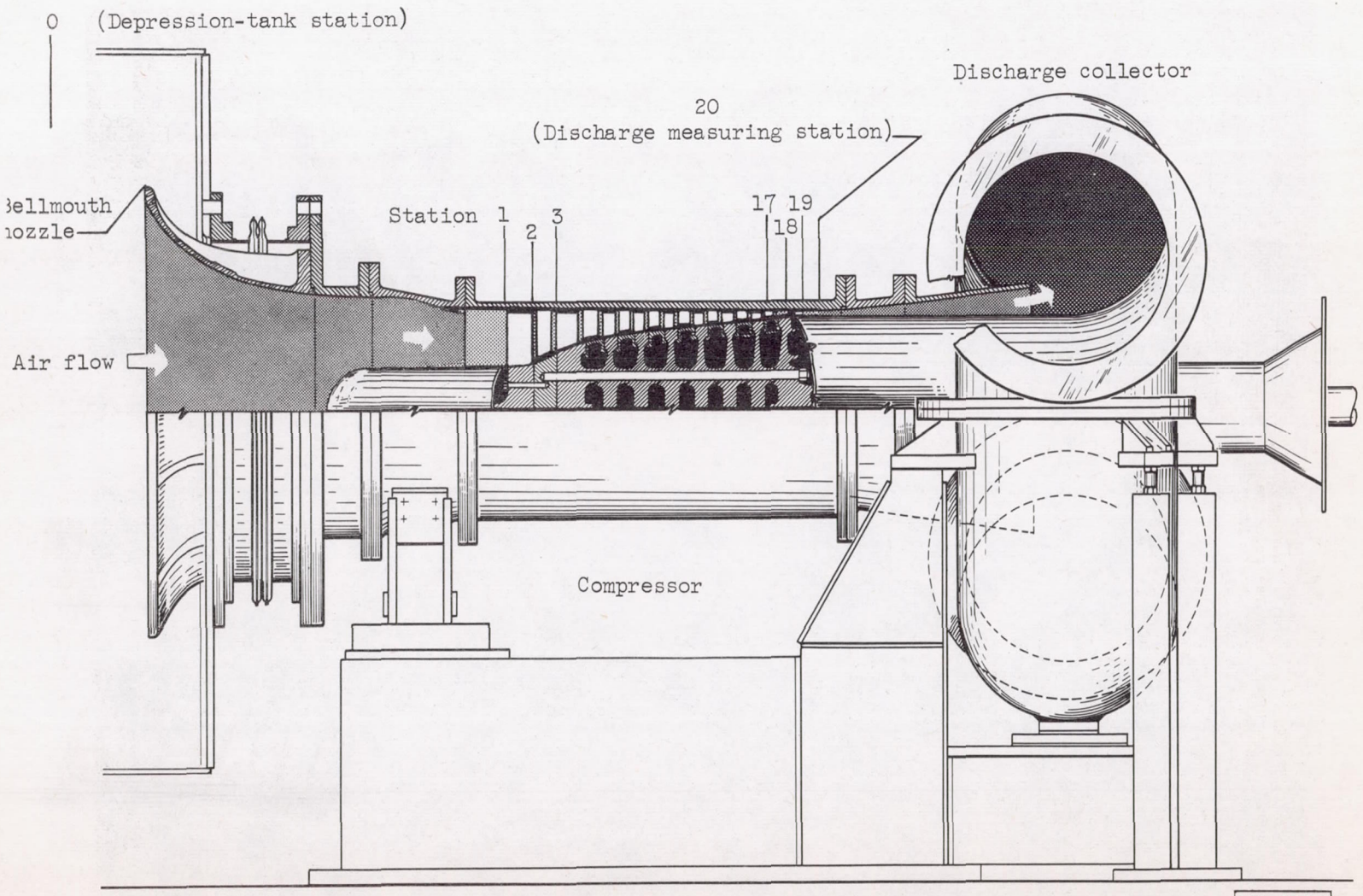
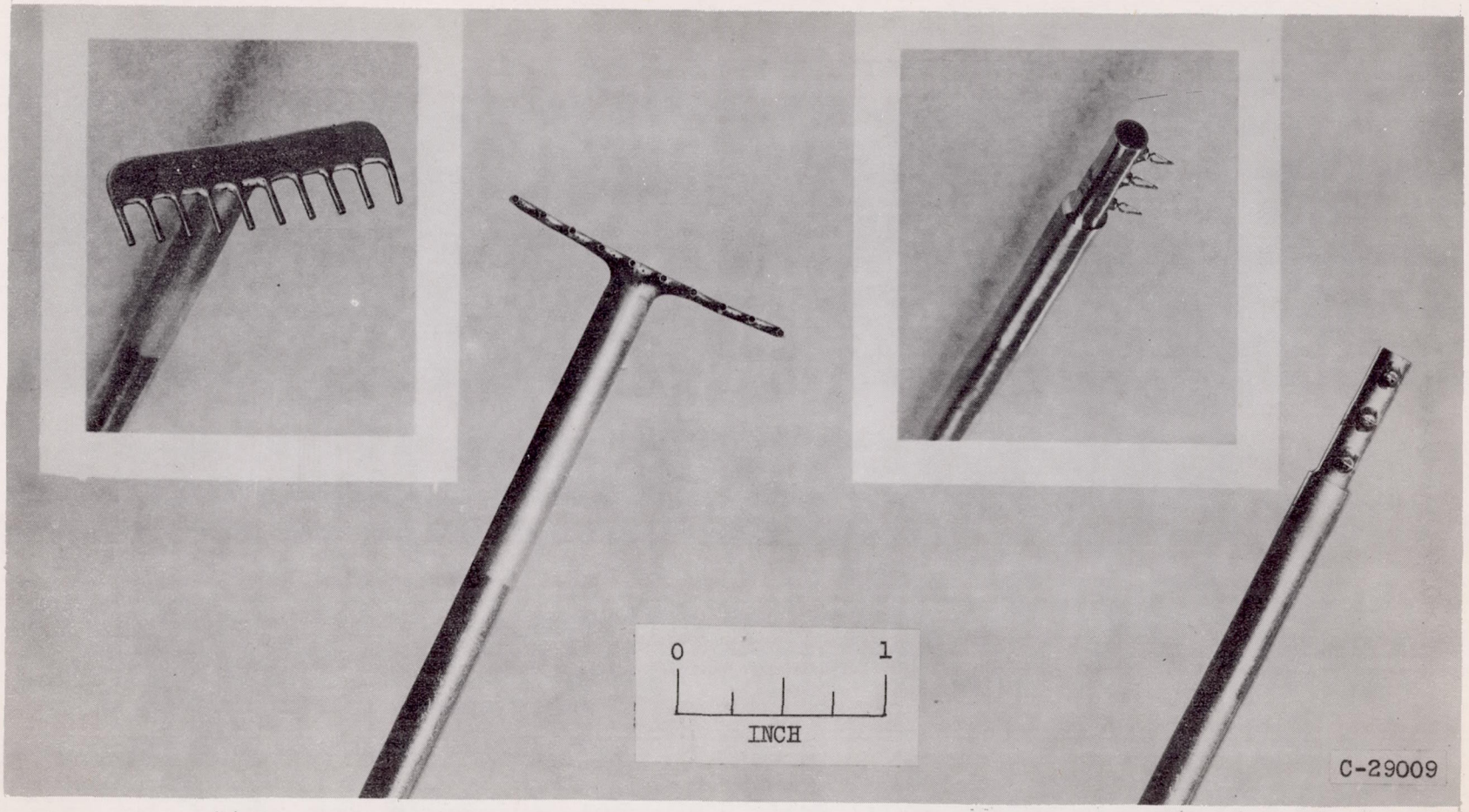



Figure 2. - Cross-sectional view of eight-stage axial-flow compressor, inlet bellmouth nozzle, and discharge collector.




(a) Total-pressure rake.

(b) Spike-type thermocouple rake.

Figure 3. - Compressor-discharge instrumentation.

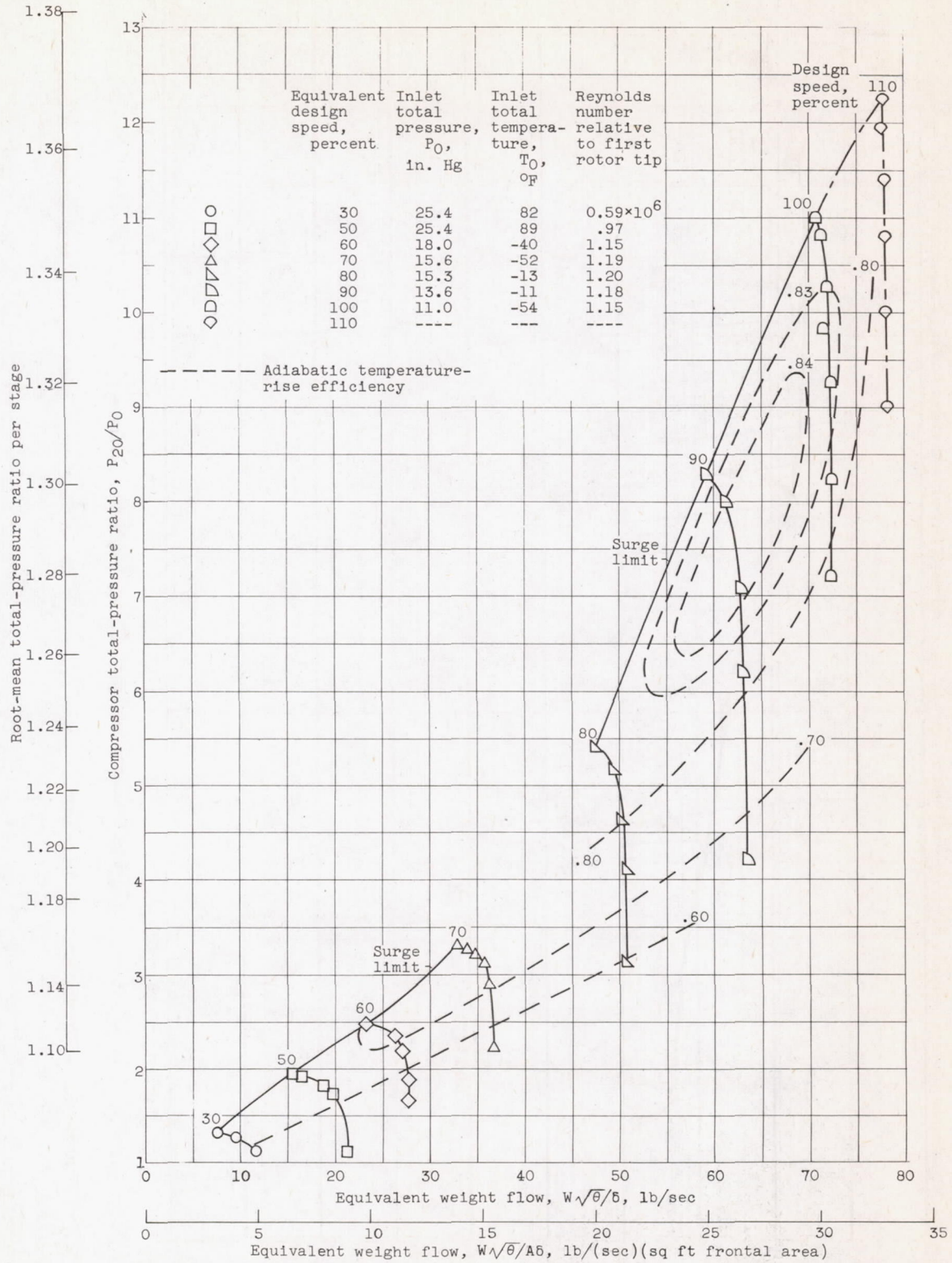



Figure 4. - Over-all performance characteristics of modified eight-stage axial-flow compressor.

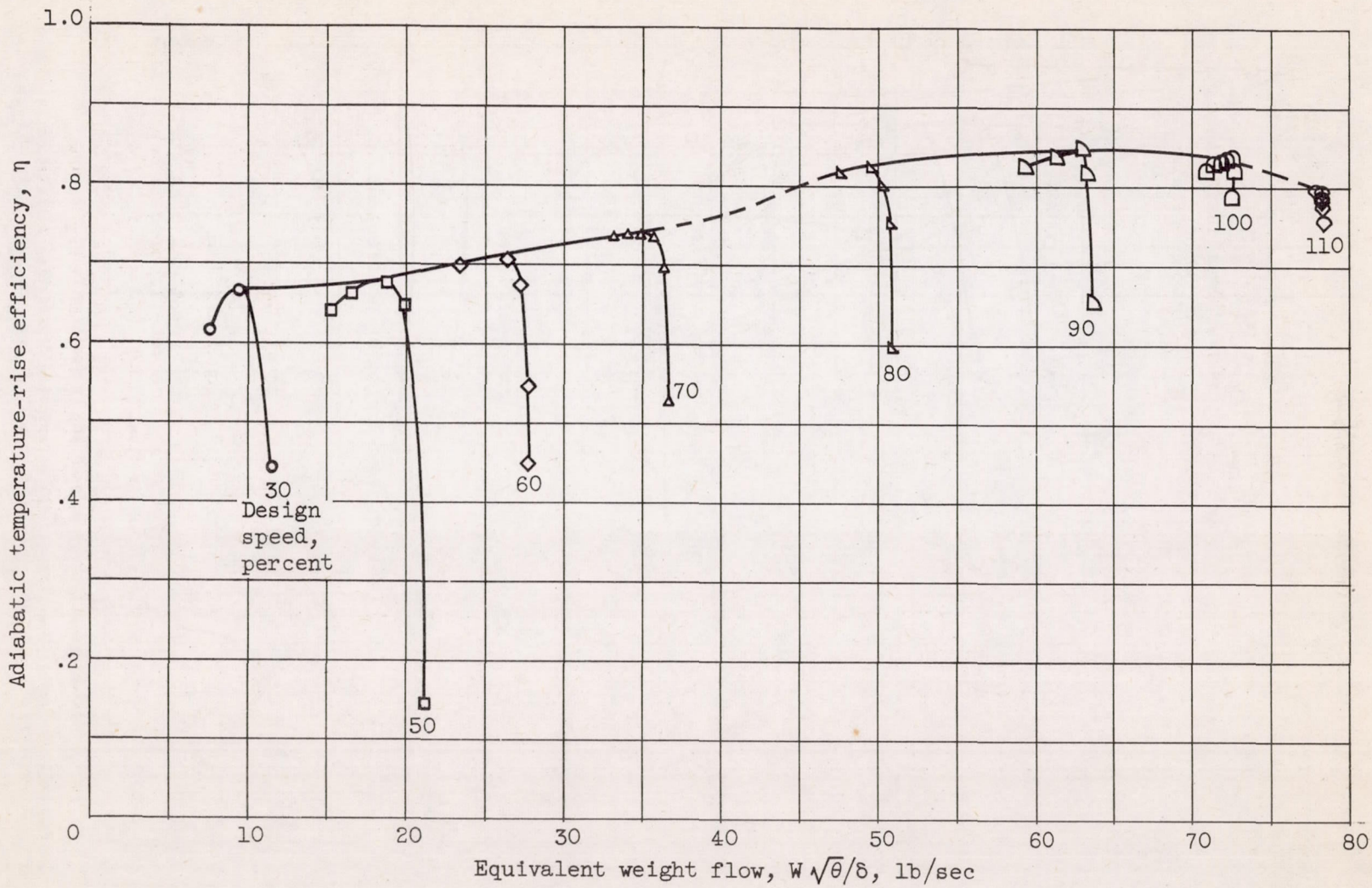



Figure 5. - Variation of adiabatic temperature-rise efficiency with speed and weight flow.

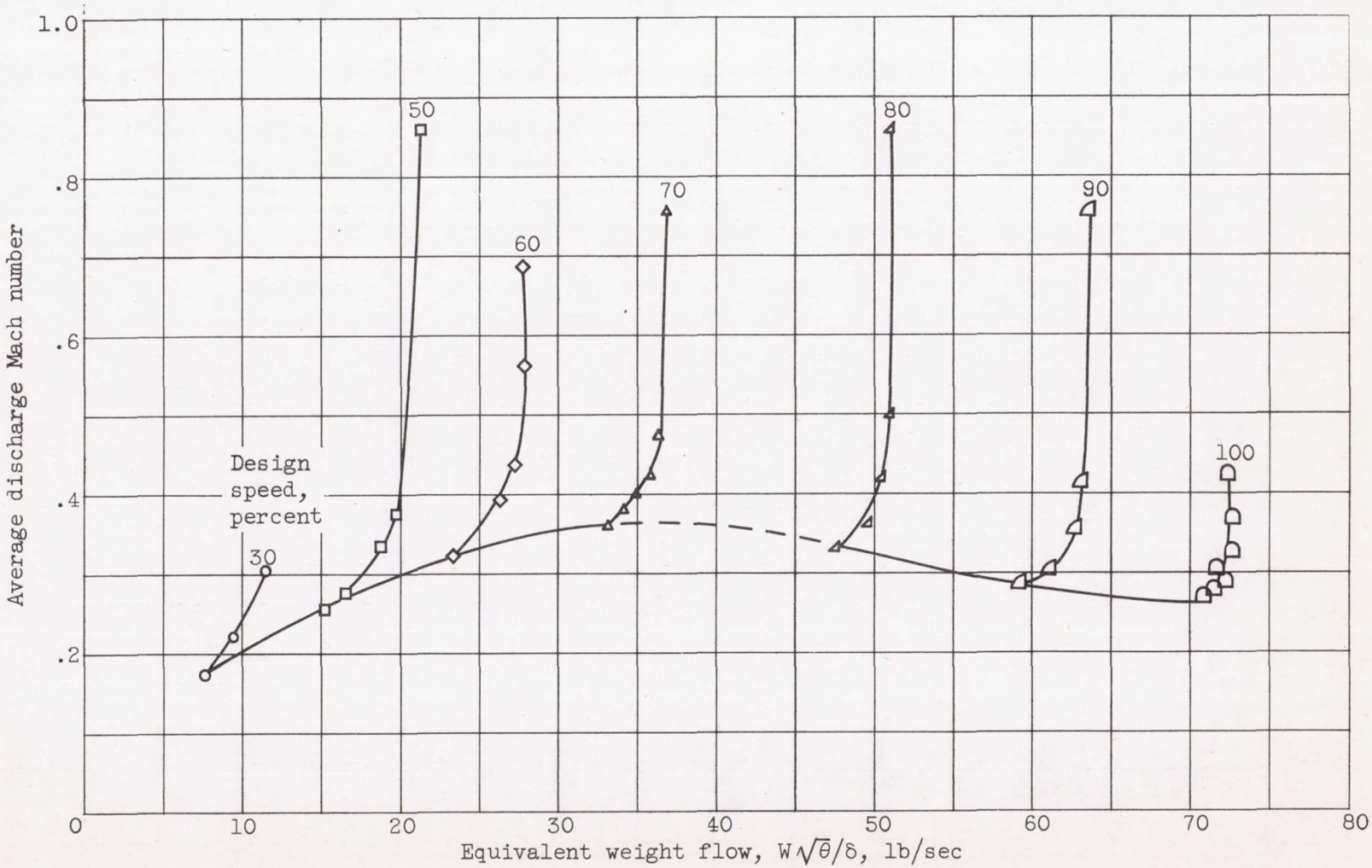



Figure 6. - Variation of average compressor discharge Mach number with speed and weight flow.

3J

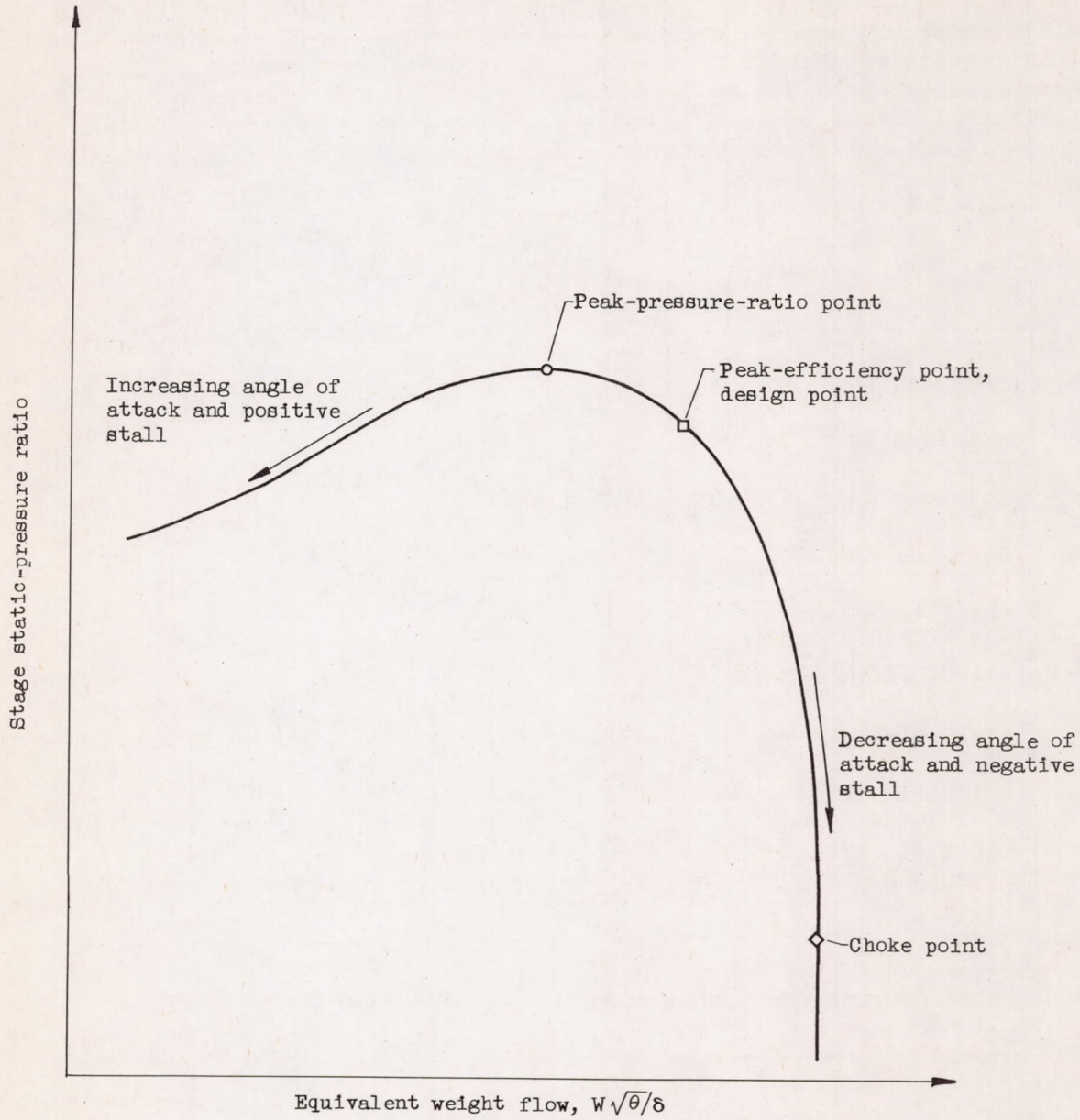
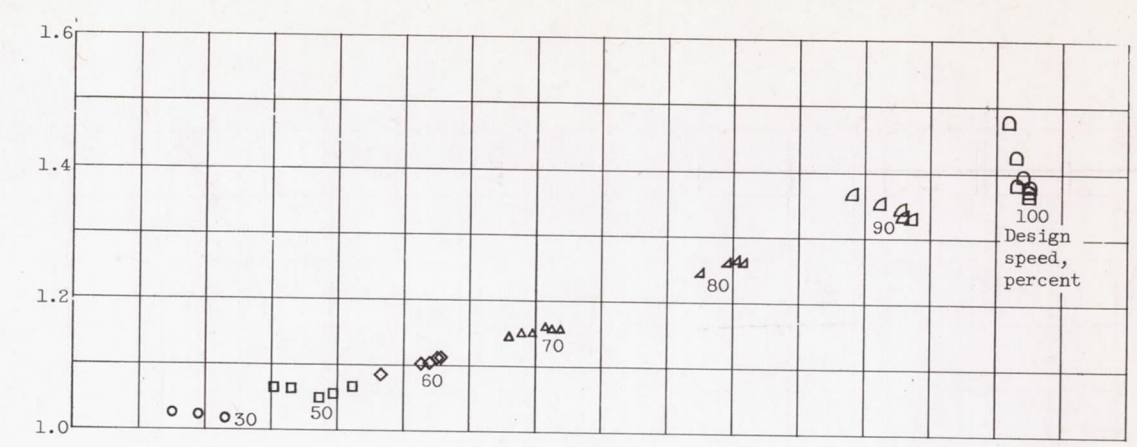
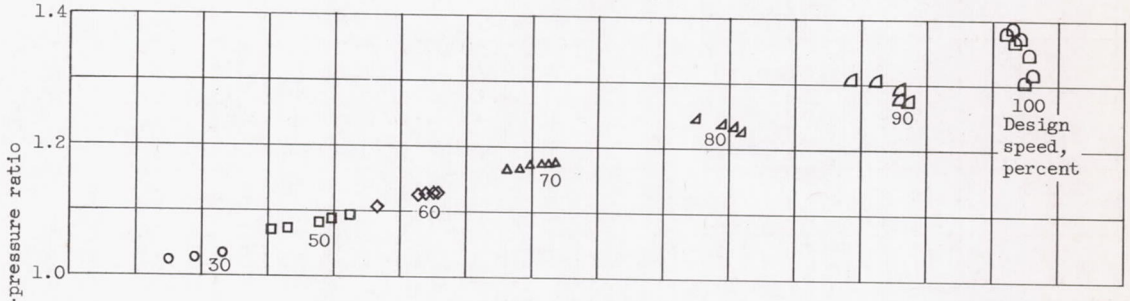


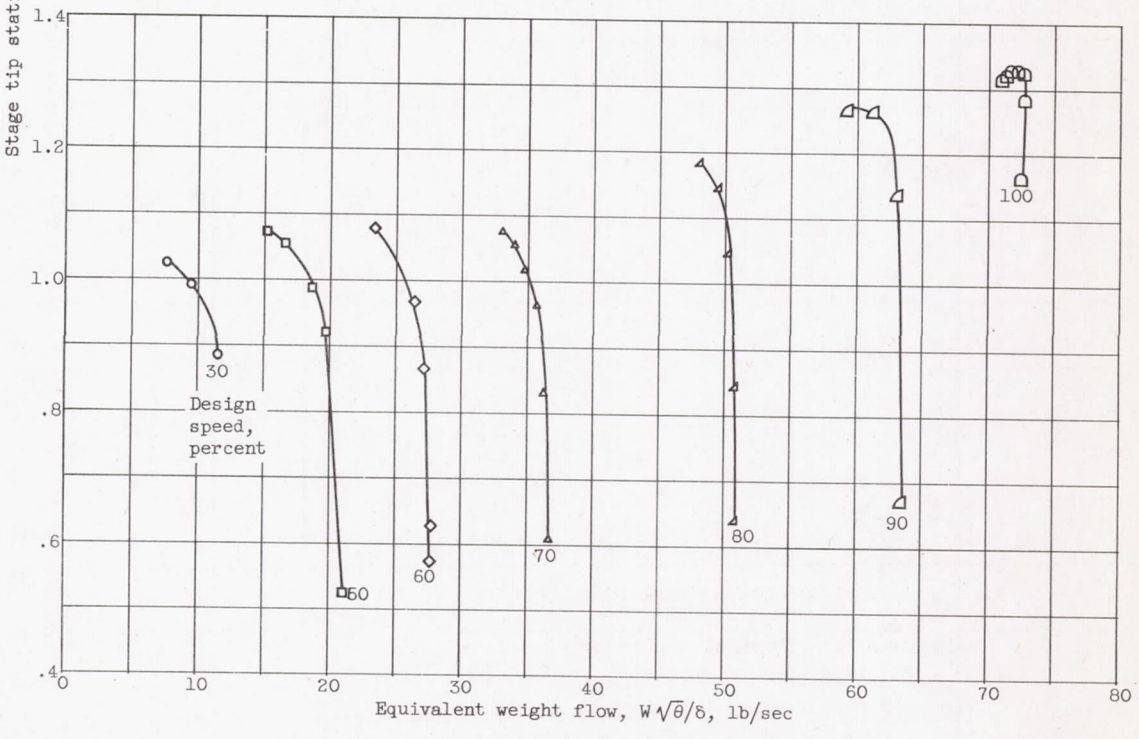

Figure 7. - Typical stage performance curve.




(a) First stage.




(b) Fourth stage.




(c) Eighth stage.

Figure 8. - Variation of stage tip static-pressure ratio across first, fourth, and eighth stages with speed and weight flow.

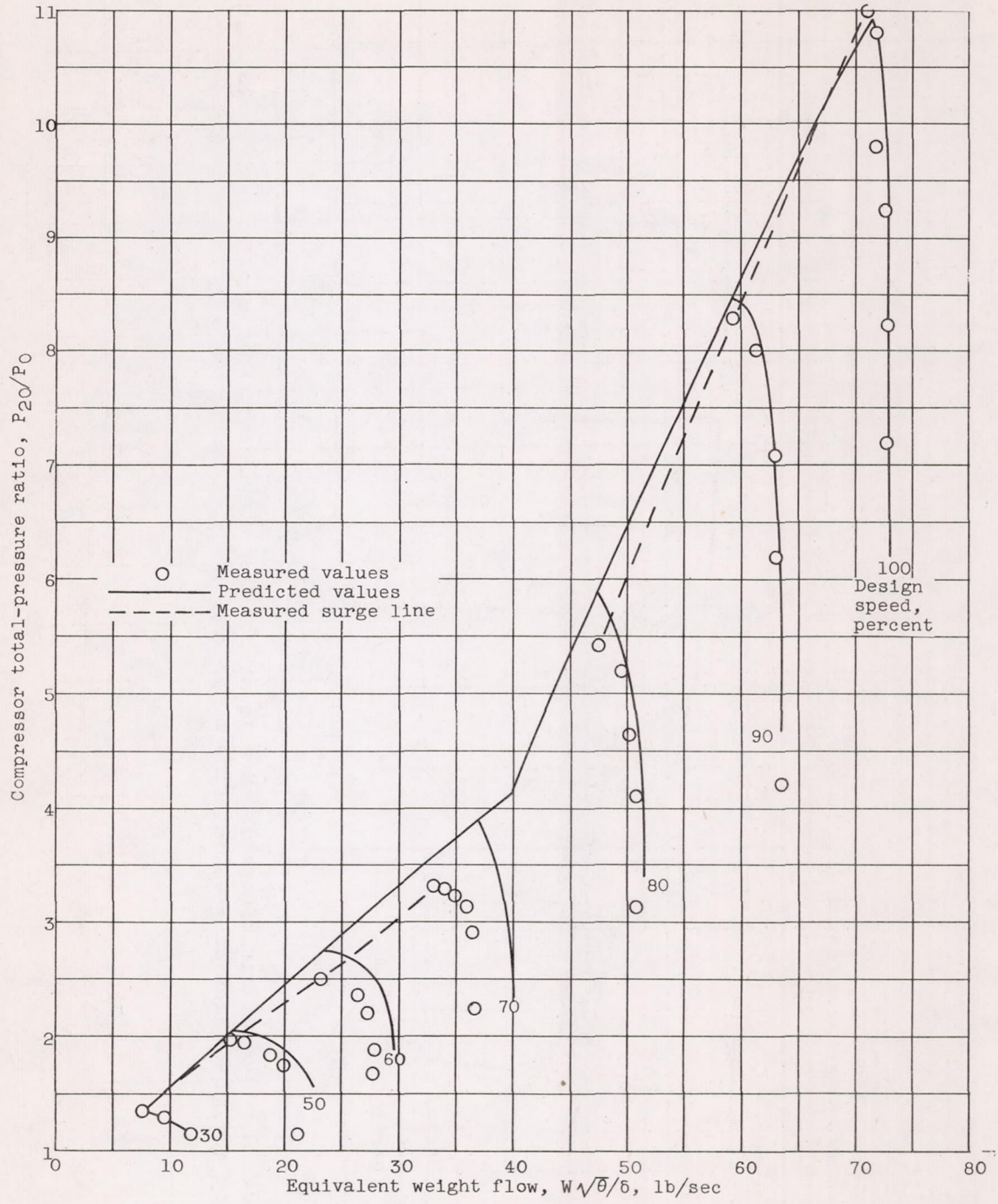



Figure 9. - Comparison of predicted over-all total-pressure ratio and weight flow with measured values for modified eight-stage axial-flow compressor.

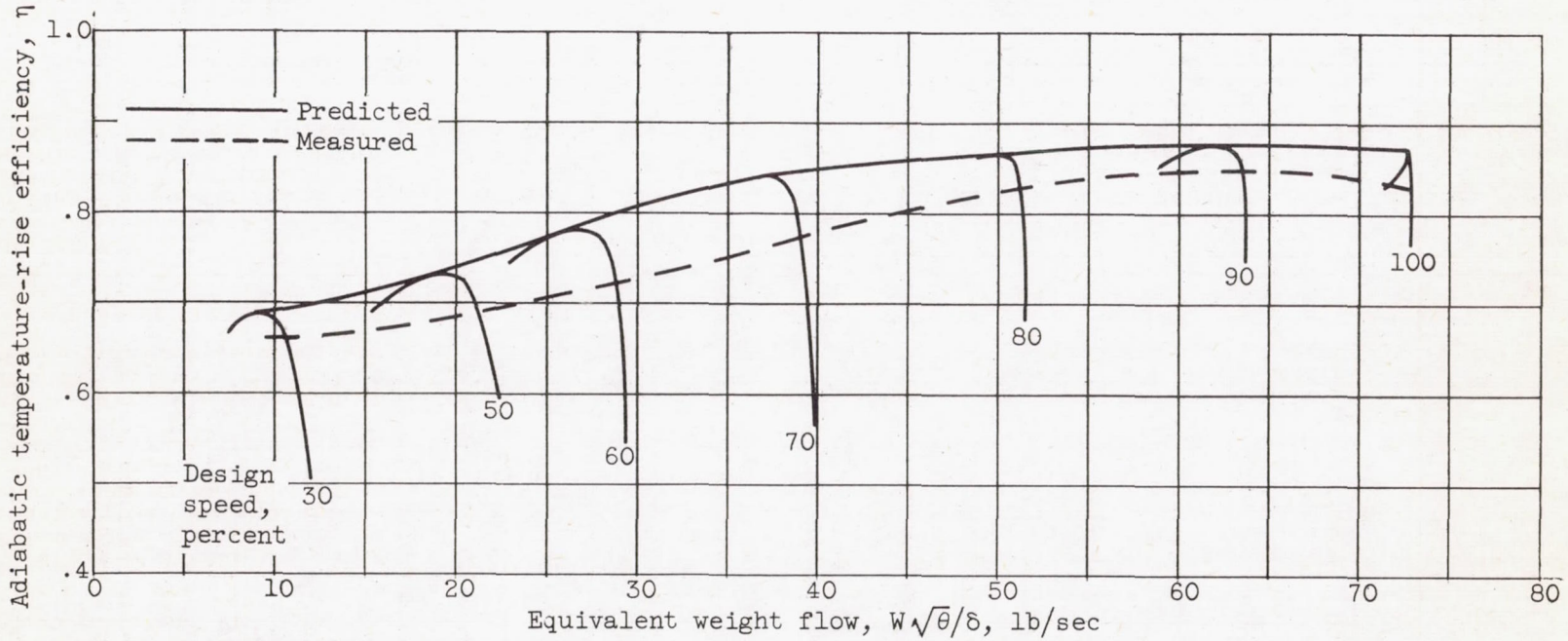



Figure 10. - Comparison of predicted adiabatic temperature-rise efficiency with measured values from modified eight-stage axial-flow compressor.